Int. J. Bio-Inorg. Hybd. Nanomat., Vol. 1, No. 4 (2012), 233-241

International Journal of Bio-Inorganic Hybrid Nanomaterials

Optical, Photoluminescence and Thermoluminescence Properties Investigation of ZnO and Mn Doped ZnO Nanocrystals

Meysam Mazhdi[1*], Faramarz Torkzadeh[2], Faezeh Mazhdi[3]

[1] Department of Physics, Faculty of Sciences, I.H.U, Tehran, Iran

[2] Department of Physics, Faculty of Sciences, Islamic Azad University of south Branch, Tehran, Iran

[3] Department of Electrical and Robotics Engineering, University of Shahrood Technology, Shahrood, Iran

Received: 30 September 2012; Accepted: 5 December 2012

ABSTRACT

ZnO and ZnO: Mn nanocrystals synthesized via reverse micelle method. The structural properties nanocrystals were investigated by XRD and Transmission electron microscopy (TEM). The XRD results indicate that the synthesized nanocrystals had a pure wurtzite (hexagonal phase) structure. The various optical properties of these nanocrystals such as optical band gap energy, refractive index, dielectric constants and optical conductivity have been analyzed by using UV-Vis data. The refractive index decreases from 2.35 to 1.35 with the change of wavelength. The optical conductivity supports the accuracy of our energy band gap calculation. Room-temperature photoluminescence spectra of all the samples showed four main emission bands including a strong UV emission band, a weak blue band, a week blue-green band, and a weak green band which indicated their high structural and optical quality. Moreover the samples exposed to Gama rays sources of ^{137}Cs and ^{60}Co and their thermoluminescence properties were investigated. Their thermoluminescence response as a function of dose exhibited good linear ranges, which make them very promising detectors and dosimeters suitable for ionizing radiation.

Keyword: ZnO; Reverse micelle; UV-Vis Spectroscopy; Optical properties, Photoluminescence, Thermoluminescence, Nuclear radiation detection.

1. INTRODUCTION

Semiconductor nanocrystals have attracted great applied during the past two decades. New devices with semiconductor nanocrystals may possess novel optical and electronic properties, which are potentially useful for technological applications, compared to the corresponding bulk materials

(*) Corresponding Author - e-mail: meisam.physics@gmail.com

[1-3]. Extremely high surface area to volume ratio is obtained with the decrease of particle size, which leads to an increase in surface specific active sites for chemical reactions and photon absorptions. The enhanced surface area also affects chemical reaction dynamics. The size quantization increases the energy band gap between the conduction band electrons and valence band holes which leads to change in their optical properties [3]. Zinc oxide, a typical II-VI compound semiconductor, with a direct band gap of 3.2 eV at room temperature and 60 meV as excitonic binding energy, is a very good luminescent material used in displays, ultraviolet and visible lasers, solar cells components, gas sensors and varistors [1, 2].

Recently, a number of techniques such as reverse micelle, hydrothermal, sol-gel, and wet chemical have been employed in the synthesis of zinc oxide nanocrystals [1-4]. However, the reverse micelle technique is one of the more widely recognized methods due to its several advantages, for instance, soft chemistry, demanding no extreme pressure or temperature control, easy to handle, and requiring no special or expensive equipment [4]. Thermoluminescence (TL) is widely accepted as a useful and reliable technique to study defects in semiconductors materials, but the more widely spread and successful application of the TL is in the field of radiation dosimetry. Many phosphor materials, synthetic as well as natural, have been characterized to evaluate its feasibility as thermoluminescence dosimeters (TLD), applicable in several low dose dosimetry areas, such asenvironmental dosimetry, clinical dosimetry, among others. ZnO exhibits TL under irradiation with different sources and striking radiation hardness. Moreover, ZnO is inert to environmental conditions, nontoxic and insoluble in water [5].

In this scientific work, ZnO and ZnO:Mn nanocrystals were fabricated through the reverse micelle method. The structural and optical characteristics of these nanocrystals were analyzed. The samples were exposed to Gama radiation to study their TL and dosimetric characterization and the results obtained show that these nanocrystals are very suitable as detectors and TL dosimeters.

2. EXPERIMENTAL

2.1. Preparation

ZnO and ZnO: Mn nanocrystals were fabricated through the mixture of two microemulsion systems. In microemulsion (I) butanol as oil, PVP as surfactant and zinc acetate (or zinc acetate and 1% by weight manganese acetate for ZnO:Mn nanocrystals) and water as aqueous phase were used in solution. Microemulsion (II) has similar mixture but instead of previous aqueous solution, the potassium hydroxide and water were used as aqueous media. The two microemulsion solutions (I) and (II) were mixed vigorously with a magnetic stirrer. Then centrifugation took place and the precipitation was kept at 250°C for 3 hours, till ZnO and ZnO:Mn samples were fabricated.

2.2. Characterization

Obtained nanocrystals were analyzed by X-ray diffractometer (Scifert, 3003 TT) with Cu-k_α radiation, UV-Vis spectrometer (PERKIN ELMER, Lambda 45), Transmission electron microscopic (80 keV, Zeiss, EM 900) luminescence spectrophotometer (PERKIN ELMER, LF55), Atomic absorption spectrometer (PERKIN ELMER, 1100B) and TLD reader (HARSHAW 4500).

3. RESULTS AND DISCUSSION

3.1. XRD analysis

Figure 1 shows the XRD patterns of ZnO and ZnO:Mn nanocrystals. The spectrums show three broad peaks for ZnO and ZnO:Mn at the 2θ= 31.744, 34.398, 36.223 and 2θ= 31.647, 34.313, and 36.131 positions. The three diffraction peaks correspond to the (100), (002), and (101) crystalline planes of hexagonal ZnO.

All the peaks in the XRD patterns of ZnO and ZnO: Mn samples could be fitted with the hexagonal wurtzite structure having slightly increased lattice parameter values for Mn doped sample (For ZnO nanocrystals *a*= 3.250 A°, *c*= 5.207 A° and ZnO:Mn nano-crystals, a= 3.256 A°, *c*= 5.212 A°) in comparison to that of

pristine ZnO sample (a= 3.249 A°, c= 5.205 A°, JCPDS no. 36-1451).

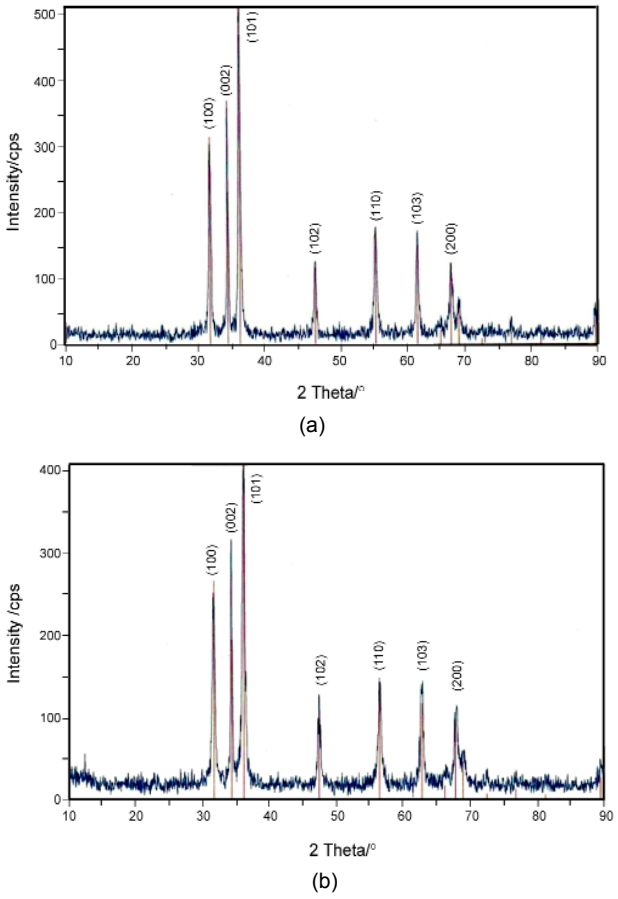

Figure 1: *XRD patterns of ZnO (a) and ZnO:Mn (b) nanocrystals.*

The increased lattice parameter values of Mn doped ZnO indicates the incorporation of manganese at zinc sites [4]. The broadening of the XRD lines is attributed to the nanocrystalline characteristics of the samples, which indicates that the crystal size is in nanometer range.

The inter planar spacing (d) is evaluated using the relation (1),

$$\frac{1}{d^2} = \frac{4}{3}\left(\frac{h^2 + hk + k^2}{a^2}\right) + \frac{l^2}{c^2} \qquad (1)$$

d-spacing for (100), (002), (101) planes is 2.8146, 2.6035, 2.4760 A° and 2.8204, 2.6062, 2.4806 A° for ZnO and ZnO:Mn nanocrystals, respectively. But, due to the size effect, the XRD peaks are broad. From the width of the XRD peak broadening, the mean crystalline size has been calculated using Scherer's equation [6]:

$$D = \frac{K\lambda}{\beta \cos\theta} \qquad (2)$$

Where D is the diameter of the particle, K is a geometric factor taken to be 0.9, λ is the X-ray wavelength, θ is the diffraction angle and β is the full width at half maximum of the diffraction main peak at 2θ. The mean crystal size of ZnO and ZnO:Mn nanocrystals resulted to be 21 and 18 nm.

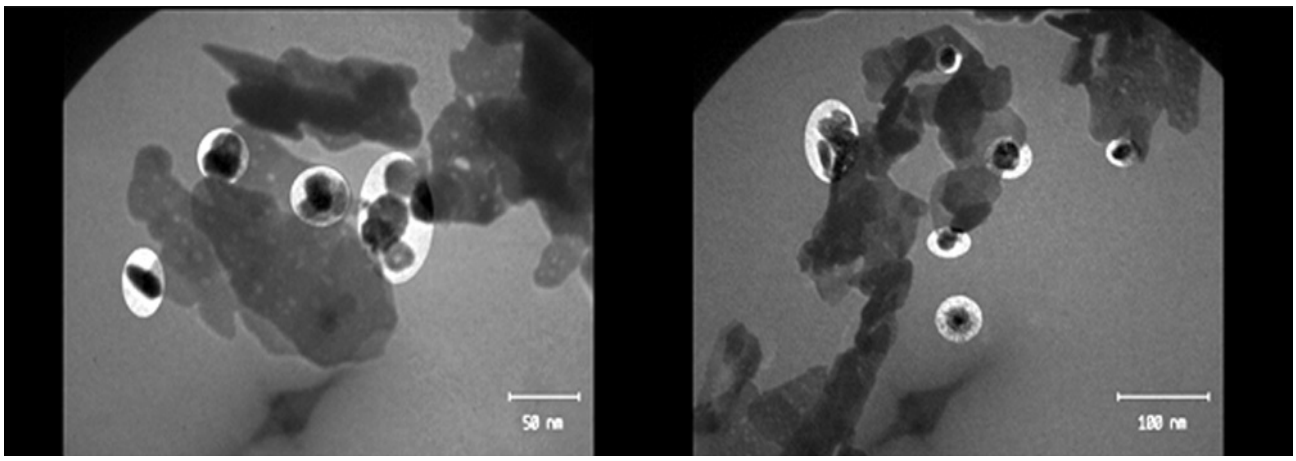

Figure 2: *TEM micrograph at high magnification and size distribution histogram of ZnO nanocrystals.*

3.2. TEM studies

TEM high magnification imaging allows the determination of size and individual crystallite morphology. TEM micrographs of the ZnO powder and size distribution histogram of nanocrystals obtained by TEM micrograph is presented in Figure 2. The main products are the spherical or quasi-spherical nanocrystals and the maximum size distribution is related to 18-23 nm.

3.3. Atomic absorption study

The atomic absorption studies confirmed attendance of manganese at zinc sites in ZnO:Mn nanocrystals. It supported the result obtained by XRD analysis. The amount of Mn doping is about 1% by weight.

3.4. Optical study

For the measurements of UV-Vis spectroscopy, we use the PVP, butanol and water as microemulsion system and nanocrystals are suspended in the emulsion. The thickness of solution in quartz glass was 1 cm. The optical characteristic of the samples is investigated from the absorption measurements in the range of 300-700 nm.

Figure 3 shows the UV-Vis absorption spectra of ZnO and ZnO:Mn nanocrystals. The excitonic absorption peak is observed due to the ZnO and ZnO: Mn nanocrystals at 310 nm, which lies much below the band gap wavelength of 388 nm of bulk ZnO [3].

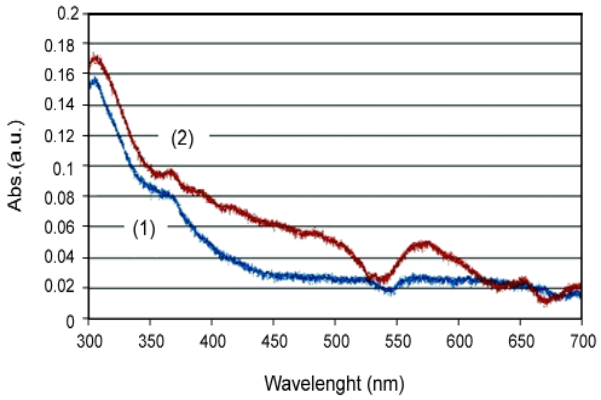

Figure 3: *UV-Vis absorption and transmission characteristics of ZnO (1) and ZnO:Mn (2) nanocrystals.*

Absorption coefficient (α) associated with the strong absorption region of the sample was calculated from absorbent (A) and the sample thickness (t) was used the relation:

$$\alpha = 2.3026\frac{A}{t} \tag{7}$$

While the optical band gap can be calculated using the following relation [7, 8]:

$$\alpha h\nu = B(h\nu - E_g)^{0.5} \tag{8}$$

Where B is a constant and E_g is the optical band gap of the material. Plot of $(\alpha h\nu)^2$ versus hν will indicate a divergence at an energy value. The estimated band gap from the plot of $(\alpha h\nu)^2$ versus hν for ZnO and ZnO: Mn nanocrystals can be seen in Figure 4.

The calculated band gap value of the ZnO and ZnO: Mn was 3.58 and 3.53 eV. The ZnO: Mn nanocrystals band gap values are lower than ZnO nanocrystals because the magnetic properties of ZnO: Mn nanocrystals increase by doped manganese and interaction potential become stronger in comparison with ZnO nanocrystals [4].

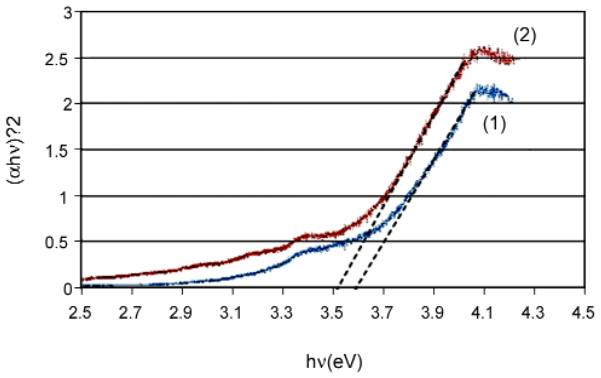

Figure 4: *The plot of $(\alpha h\nu)^2$ versus hν of ZnO (1) and ZnO:Mn (2) nanocrystals.*

The extinction coefficient for a particular substance is a measure of how well it absorbs electromagnetic radiation, or the amount of impedance the material offers for the passage of electromagnetic radiation through it. Extinction

coefficient (k) was calculated from absorption coefficient (α) using the relation where λ is the spectrum absorption wavelength:

$$k = \frac{\alpha\lambda}{4\pi} \quad (4)$$

The extinction coefficient (k) as function of photon energy is shown in Figure 5. In ultra violet wavelengths extinction of rays in nanocrystals is much more than the visible wavelengths and this value for ZnO:Mn nanocrystals are more than ZnO nanocrystals.

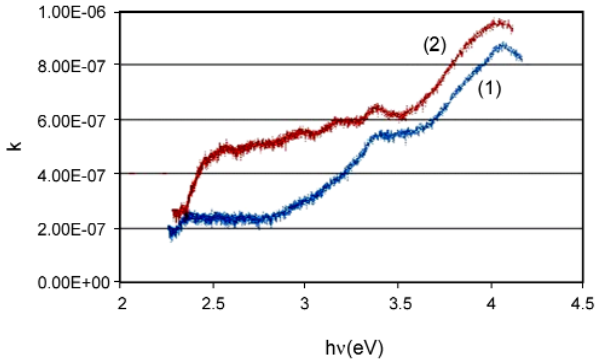

Figure 5: *Extinction coefficient (k) as function of the photon energy for ZnO (1) and ZnO:Mn nanocrystals (2).*

The refractive index of a substance is a measure of the speed of light in that substance. It is expressed as a ratio of the speed of light in vacuum relative to that in the considered medium. The refractive index has been calculated using the following relation,

$$n = \left(\frac{1+R}{1-R}\right) + \sqrt{\left(\frac{4R}{(1-R)^2} - k^2\right)} \quad (5)$$

Where k is the extinction coefficient and R is the optical reflectance [9]. The transmittance (T) can be calculated from the relationship $A=\log 1/T$, Where A is the absorbance and T is given by $T=1/10^A$. Optical reflectance (R) is calculated from the relation $R=1-(A+T)$ [10].

The variation of refractive index with wavelength for nanocrystals is shown in Figure 6. It is evident that the refractive index decreases from 2.35 to 1.35 with the change of wavelength which is in good agreement with those reported by other researchers.

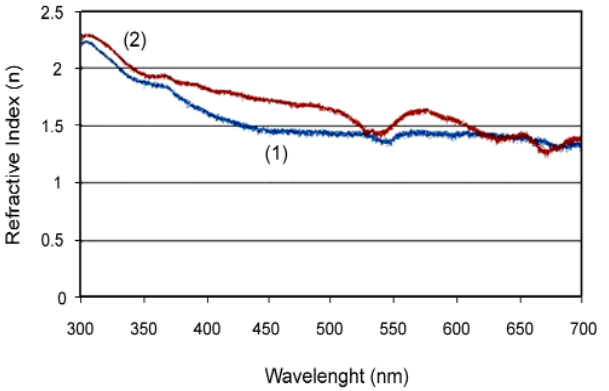

Figure 6: *Variation of refractive index as a function of wavelength for ZnO (1) and ZnO:Mn (2) nanocrystals.*

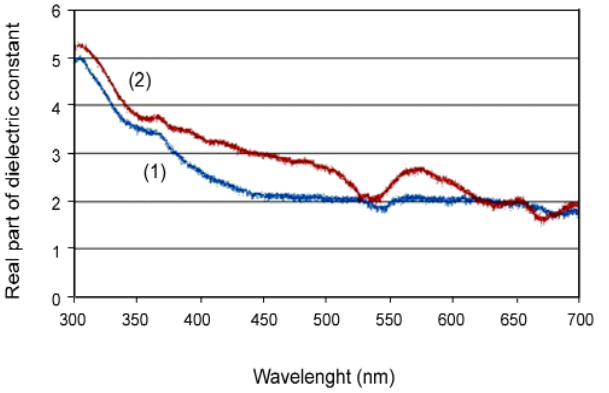

Figure 7: *Variation of Real part of dielectric constants as a function of wavelength for ZnO (1) and ZnO:Mn (2) nanocrystals.*

The dielectric constant is the ratio of the permittivity of a substance to the permittivity of free space. It is an expression of the extent to which a material concentrates electric flux, and is the electrical equivalent of relative magnetic permeability. The real ε_r and imaginary ε_i parts of the dielectric constant were determined using the formula $\varepsilon_r=n^2-k^2$ and $\varepsilon_i=2nk$ [9]. The variation of the real (ε_r) and imaginary (ε_i) parts of the dielectric constant for nanocrystals are illustrated in

Figures 7 and 8. The Figures revealed that the values of the real part are higher than the imaginary part. From the optical data, it is observed that refractive index (n), the extinction coefficient (k), the real (ε_r) and imaginary (ε_i) parts of the dielectric constant follow the same pattern.

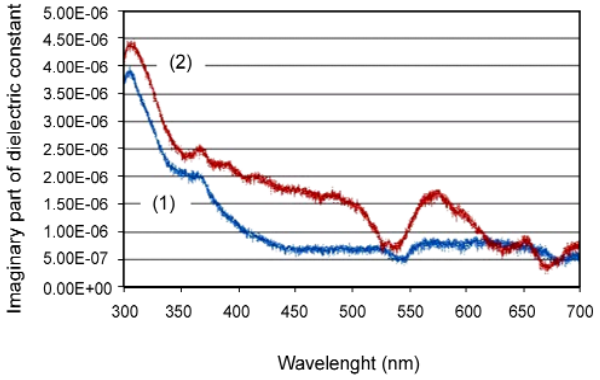

Figure 8: *Variation of Imaginary part of dielectric constants as a function of wavelength for ZnO (1) and ZnO:Mn (2) nanocrystals.*

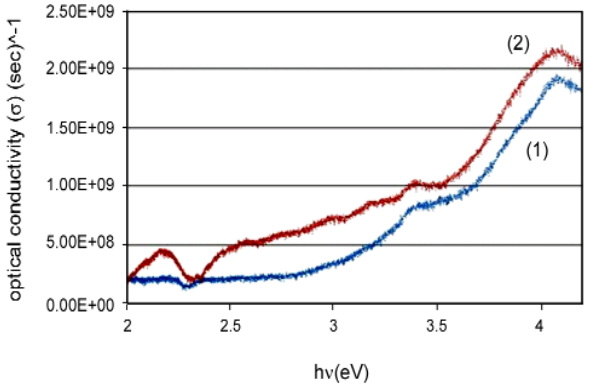

Figure 9: *Plot of optical conductivity as a function of photon energy (eV) for ZnO (1) and ZnO:Mn (2) nanocrystals.*

Optical conductivity is one of the powerful tools for studying the electronic states in materials. If a system is subjected to an external electric field then, in general, a redistribution of charges occurs and currents are induced. For small enough fields, the induced polarization and the induced currents are proportional to the inducing field. The optical conductivity σ was calculated using the following relation [Srivastava et al, 2009]:

$$\sigma = \frac{\alpha n c}{4\pi} \qquad (6)$$

The optical conductivity of the nanocrystals for larger energy values is observed as an exponential increase (Figure 9). This can be explained in terms of the transfer of a large number of charge carriers from the valence to conduction band in ZnO and ZnO:Mn nanocrystals. Thus a sudden rise in optical conductivity observed at 3.5 eV supports the accuracy of energy band gap calculation [10].

3.5. Photoluminescence study

Room temperature PL spectra of the ZnO and ZnO:Mn nanocrystals samples are shown in Figure 10.

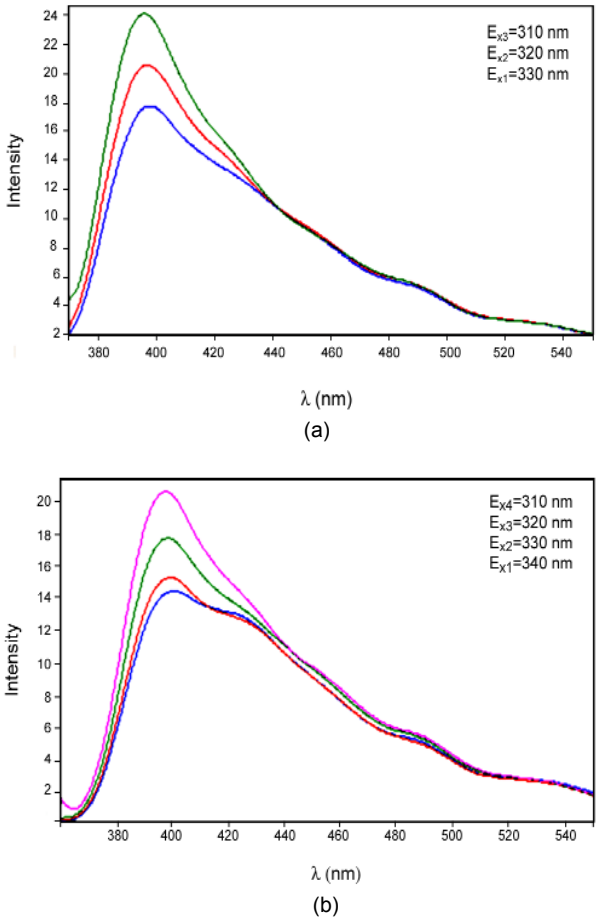

Figure 10: *Room temperature photoluminescence spectra of ZnO (a) and ZnO:Mn (b) nanocrystals.*

The spectra of nanocrystals mainly consist of four emission bands: a strong UV emission band at ~400 and 395 nm, a weak blue band at ~450 and 445 nm, a weak blue-green band at ~490 and 485 nm and a very weak green band at ~530 and 525 nm for ZnO and ZnO:Mn nanocrystals. The strong UV emission corresponds to the exciton recombination related near-band edge emission of ZnO. The weak blue and weak blue-green emissions are possibly due to surface defects in the nanocrystals as in the case of ZnO nanomaterials reported by other researchers. The weak green band emission corresponds to the singly ionized oxygen vacancy in ZnO, and this emission results from the recombination of a photogenerated hole with the singly ionized charge state of the specific defect. The low intensity of the green emission ZnO nanocrystals may be due to the low density of oxygen vacancies during the preparation than the ZnO:Mn nanocrystals, where as the strong room-temperature UV emission intensity should be attributed to the high purity with perfect crystallinity of the synthesized ZnO nanocrystals [1].

3.6. Thermoluminescence study

Figure 11 shows the intensity of thermoluminescence effect of nanocrystals at different times and under the irradiation of visible light. Thermoluminescence intensity has increased by increase of irradiation time for both samples. Samples are pure zinc oxide nanocrystal and doped zinc oxide nanocrystal by manganese that are labeled by number 1 and 2 at the Figure 11 respectively. Sensibility of pure zinc oxide nanocrystal to visible light is more than zinc oxide nanocrystal that doted by manganese.

Figure 12 shows the intensity of thermoluminescence effect of nanocrystals without irradiation of visible light and under the irradiation of gamma rays of cesium source. By reason of sensibility of samples to visible light, when irradiate samples put them in thin black plastic shielding therefore by this method, effect of visible light on thermoluminescence intensity has omitted. The exposure intensity of cesium source at the distance of 50 cm is 10 mSv that by putting samples at this distance and access

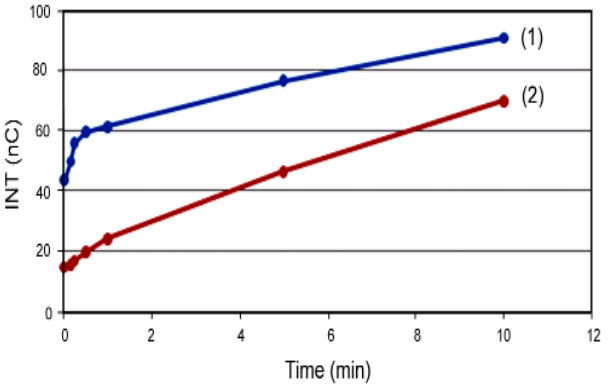

Figure 11: *Intensity of thermoluminescence effect of nanocrystals at different times and irradiation of visible light for ZnO (1) and ZnO:Mn (2).*

of exposure time, the rate of nanocrystals exposure will increase. Thermoluminescence treatment of nanocrystals at the doses between 5-30 mSv is linear and gradient of this line indicate the calibration coefficient. The calibration coefficient for pure and doped zinc oxide is 1.74 ± 0.11 nC/gr.mSv and 1.90 ± 0.14 nC/gr.mSv respectively.

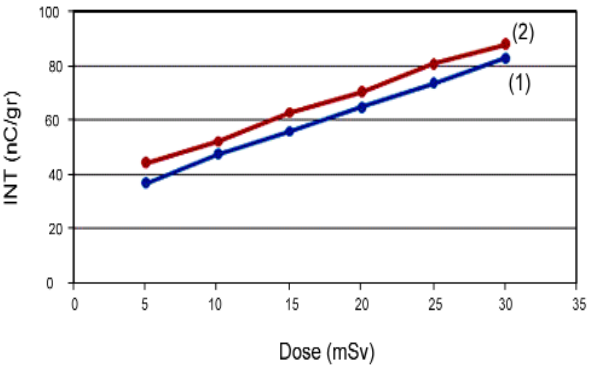

Figure 12: *Intensity of nanocrystals thermoluminescence treatment for ZnO (1) and ZnO:Mn (2) by irradiation of gamma rays of cesium source versus exposure dose.*

Figure 13 shows intensity of nanocrystals thermoluminescence treatment versus exposure dose by distance changing without visible irradiation but against of gamma rays of cobalt source. The calibration coefficient for pure and doped zinc oxide at the range of 0.62 - 21.74 Sv is 7.87 ± 0.18 nC/gr.Sv and 8.50 ± 0.15 nC/gr.Sv respectively.

Figure 14 shows intensity of nanocrystals thermoluminescence treatment without visible irradiation but against of gamma rays of cobalt source. By putting samples at constant distance of source and access of their exposure time (i.e. between 1-8 hours), the rate of nanocrystals exposure will increase between 21.74 - 173.90 Sv. The calibration coefficient for pure and doped zinc oxide at the range of is 6.19 ± 0.15 nC/gr.Sv and 13.84 ± 0.21 nC/gr.Sv respectively. Therefore the sensitivity of doped zinc oxide nanocrystals by manganese to gamma rays is more than the pure ones.

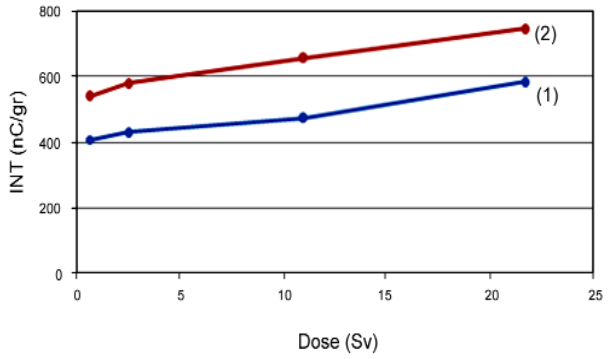

Figure 13: *Intensity of nanocrystals thermoluminescence treatment for ZnO (1) and ZnO: Mn (2) by irradiation of cobalt source versus exposure dose.*

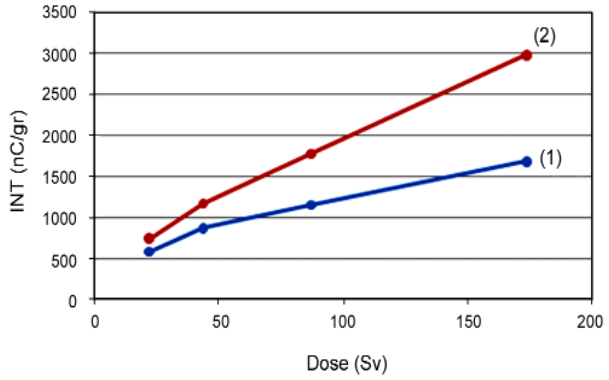

Figure 14: *Intensity of nanocrystals thermoluminescence treatment for ZnO (1) and ZnO: Mn (2) by irradiation of cobalt source versus exposure dose.*

By comparison of calibration coefficient we achieve to this result that thermoluminescence response of doped zinc oxide nanocrystals by manganese is more than pure zinc oxide nanocrystals and also thermoluminescence response of zinc oxide nanocrystals to gamma rays at overdose is more than median dose. The fading of thermoluminescence response decreasing is by reason of some trapped charge between compietion of exposure and reading and this is due to light and thermal fading. For the restriction of light fading, we put the nanocrystals in opaque covers.

Figure 15 shows fading percent of nanocrytals thermoluminescence intensity until to 10 days after first reading. Fading intensity decreases by increasing the duration between readings and decrease of chart gradient. Thereupon fading velocity at the first days after exposure is very high that by increase the duration between exposure and reading, this process decrease.

Fading treatment of pure and doped nanocrystals thermoluminescence intensity is similar to each other but fading rate of pure sample is more than doped. The reason of this treatment can be explained in effect of capturing new deep centers. These centers have created by incoming manganese as impurity in nanocrystal lattice. Thereupon captured charges for doped samples have more thermal stability than pure ones, as this reason has corresponding to light sensitivity treatment of samples and have shown in Figure 11.

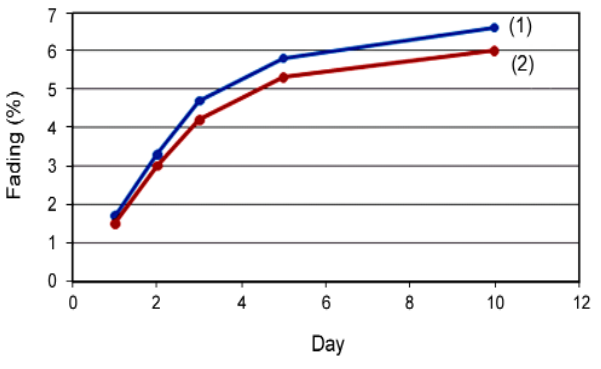

Figure 15: *Fading percent of nanocrystals thermoluminescence intensity for ZnO (1) and ZnO:Mn (2) by irradiation of cobalt source versus duration between exposure and reading.*

4. CONCLUSIONS

ZnO and ZnO:Mn nanocrystals with hexagonal structure have been synthesized by the reverse micelle method using PVP as surfactant. The XRD studies and TEM of these nanocrystals revealed that their average size is about 21 and 18 nm for ZnO and ZnO:Mn nanocrystals respectively. The atomic absorption studies confirmed existence of manganese at Zinc sites in ZnO:Mn nanocrystals. Also, the UV-Vis studies revealed that their optical band gap energy is 3.53 and 3.58 eV for ZnO and ZnO:Mn nanocrystals respectively. The refractive index decreases from 2.35 to 1.35 with the change of wavelength. The optical conductivity supports the accuracy of our energy band gap calculation. Room-temperature photoluminescence spectra of the samples showed four main emission bands including a strong UV emission band, a weak blue band, a week blue-green band, and a weak green band which indicated their high structural and optical quality. Doping the zinc oxide nanocrystals by manganese lead to make a single trap in crystal lattice and decrease in activation energy and these two factors result to improvement of thermoluminescence attribute and response sensitivity increase under gamma ionization radiation. Therefore add manganese as activator lead to crystal luminescence improvement. Nanocrystals thermoluminescence response as a function of exposure dose can be used for detection and dosimeter of ionizing radiation.

ACKNOWLEDGMENT

The financial support of the Laboratory at the Department of Physics in Imam Hossein University is gratefully acknowledged.

REFERENCES

1. Maensiri S., Masingboon C., Promarak V., Seraphin S., *Optical Materials*, **29**(2007), 1700.
2. Kumar D., Kumar S., Bhatti H.S., Gupta A., Sharma J.K., *Journal of Ovonic Research*, **4**(2008), 101.
3. Kumbhakar P., Singh D., Tiwary C.S., Mitra A.K., *Chalcogenide letters*, **5**(2008), 387.
4. Jayakumar O.D., Gopalakrishnan I.K., Kadam R.M., Vinu A., Asthana A., Tyagi A.K., *Journal of Crystal Growth*, **300**(2007), 358.
5. Cruz-Vazquez C., Bernal R., Burruel-Ibarra S.E., Grijalva-Monteverde H., Barboza-Flores M., *Optical Materials*, **27**(2005), 1235.
6. Khorsand Zak A., Abd. Majid W.H., Abrishami M.E., Yousefi R., *Solid State Sciences*, **13**(2011), 251.
7. Ilican S., Caglar Y., Caglar M., *Journal of optoelectronics and advanced materials*, **10**(2008), 2578.
8. Islam M.R., Podder J., *Cryst. Res. Technol*, **44**(2009), 286.
9. Srivastava M., Ojha A.K., Chaubey S., Materny A., *Journal of Alloys and Compounds* **481**(2009), 515.